

Stimulated Raman adiabatic passage in molecular electronic states

Chuan-Cun Shu, Jie Yu, Kai-Jun Yuan, Wen-Hui Hu, Jing Yang, and Shu-Lin Cong*

Department of Physics, Dalian University of Technology, Dalian 116024, China

(Received 27 November 2008; published 17 February 2009)

We explore theoretically the rovibrational dynamics of stimulated Raman adiabatic passage (STIRAP) in molecular electronic states including both the rotational and the vibrational degrees of freedom, with the LiH molecule as an example. By using a pure rovibrational state as initial state, we find that, under the condition of two-photon resonance, an efficient rovibrational population transfer can be achieved via STIRAP in molecular electronic states and the desired target state can be selected by adjusting laser-pulse parameters. Besides the interested rovibrational states, however, some unwanted rovibrational states may affect population transfer process, especially while the two-photon detuning is taken into account. By inspecting the evolution process of wave packet, we can easily search these unwanted rovibrational states and study their influences. Moreover, the effect of rotational temperature on the population transfer process is discussed using thermal mixed state as initial state.

DOI: [10.1103/PhysRevA.79.023418](https://doi.org/10.1103/PhysRevA.79.023418)

PACS number(s): 33.80.Be, 42.65.Dr, 33.20.Vq, 33.20.Fb

I. INTRODUCTION

Preparation of well-defined quantum states for atoms or molecules is an important topic in quantum optics, atomic and molecular physics, quantum information processing, and contemporary laser physics [1–3]. Controlling population transfers of atoms or molecules by strong laser pulses has also attracted attention of researchers [4–7]. Several approaches are theoretically proposed to realize this goal by pulse timing control, multipath interference, optimal control, and adiabatic passage [8–12]. The stimulated Raman adiabatic passage (STIRAP) technique, which was proposed and experimentally carried out by Bergmann and co-workers [13,14], is one of efficient ways used for controlling population transfer with two counterintuitive and partially overlapping laser beams. The STIRAP method has been widely studied, both in atomic and molecular systems with a three-level or multilevel structure [15–18].

Initially, the STIRAP was developed to steer efficiently the rovibrational excitation of molecules with continuous wave (cw) laser beams [14]. Since the transition dipole moments of many molecules are too small, currently available cw lasers are not powerful enough to induce sufficiently a larger Rabi frequency for successful application of STIRAP. Therefore, it is of significant interest to explore the feasibility of STIRAP with laser pulses. Recently, manipulation of rovibrational wave-packet composition has been studied both theoretically and experimentally with laser pulses [19–22]. Chang and Solá [23] studied the Raman excitation of rovibrational coherent and incoherent states using long pulses with bandwidth (frequency width) much less than the rotational constant. However, molecular process is very complicated due to the presence of the nuclear motion. When laser field is strong but still insufficiently intense to cause multiple ionization of molecules, the bound electronic states will be significantly modified by the laser field. These modified potential-energy surfaces will in turn affect the motion of the

nuclei [12]. Therefore, it has to be kept in mind that, for longer laser-molecule interaction time, the motion of nuclei will play an important role in excitation process because the electric dipole moment function depends on the vibrational coordinate R . On the other hand, since molecule has a lot of vibrational and rotational energy levels in each electronic state, and these rovibrational levels are very congested, some unwanted transitions among different rovibrational states may occur. In addition, if the bandwidth of laser pulse is large enough, the situation will become more complex: the field may induce the population transfer from an initial state to more rovibrational states. Therefore, it is not appropriate to explore these complicated processes by using a simple level model. Based on this consideration and the recent investigation of vibrational population transfer between molecular electronic states [24], we think that a more detailed theoretical description of STIRAP including both the rotational and the vibrational degrees of freedom is necessary.

In the framework of the Born-Oppenheimer approximation (BOA), the time-dependent quantum wave-packet method is very efficient and successful for dynamics calculations of diatomic and triatomic molecules. An attractive aspect is that much insight can be obtained by inspecting snapshots of the wave packet at regular time intervals. From the snapshots, it is easy to visualize the nuclear motion and the underlying physics. In the present work, we explore the rovibrational dynamics of STIRAP in molecular electronic states, taking the LiH molecule for example. The molecular vibration and rotation are taken into account in the calculation, and the effect of unwanted rovibrational states on STIRAP is examined in detail. We also discuss the effect of temperature on the rovibrational wave-packet manipulation using thermal mixed state as initial state.

The rest of this paper is organized as follows. In Sec. II, we summarize a standard model of STIRAP in a three-level system and introduce the theoretical treatment of STIRAP in molecular electronic states. The results and discussions are demonstrated in Sec. III. Finally, some conclusions and future perspective are given in Sec. IV

*shlcong@dlut.edu.cn

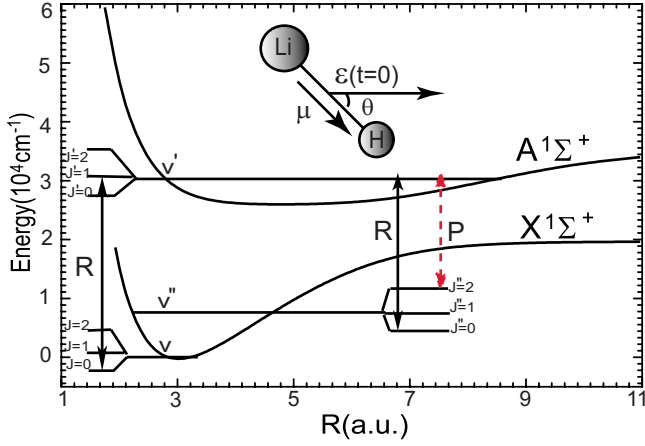


FIG. 1. (Color online) Potential-energy curves and rovibrational levels of the ground $X^1\Sigma^+$ and excited $A^1\Sigma^+$ states of the LiH molecule. The solid and dashed arrows represent the R and P branches the Raman transition, respectively.

II. THEORETICAL TREATMENTS

Figure 1 shows the Raman excitation process for one-photon-allowed rovibrational transitions in the lowest two electronic states of the LiH molecule. The pump laser couples the ground rovibrational state $|g\rangle = X^1\Sigma^+(\nu, J, M)$ to the intermediate rovibrational state $|e\rangle = A^1\Sigma^+(\nu', J', M)$, and the Stokes pulse couples the state $|e\rangle = A^1\Sigma^+(\nu', J', M)$ to final rovibrational state $|f\rangle = X^1\Sigma^+(\nu'', J'', M)$. For convenience, the ground electronic state $X^1\Sigma^+$ and the excited electronic state $A^1\Sigma^+$ are abbreviated to X and A , respectively. The total laser fields $\epsilon(t)$ is expressed as

$$\epsilon(t) = \sum_{k=P,S} E_k f_k(t) \cos[\omega_k(t - t_k)], \quad (1)$$

where E_k , $f_k(t)$, t_k , and ω_k are the field amplitude, normalized pulse envelope, center time, and carrier frequency of the k th pulse, respectively. The subscripts P and S represent the pump and the Stokes laser pulses, respectively.

When linearly polarized laser pulses are used to excite the molecule, the allowed coupling between two rovibrational levels is determined by $\langle \nu', J', M | \mu | \nu, J, M \rangle = \mu_{\nu, \nu'} \beta_{J, M}^{J', M} \delta_{J, J' \pm 1} \delta_{M, M}$, where δ is the Delta Kronecker and $\mu_{\nu, \nu'}$ is the transition dipole moment between two vibrational states. The angular overlaps are calculated by

$$\beta_{J, M}^{J-1, M} = \beta_{J-1, M}^{J, M} = \sqrt{\frac{J^2 - M^2}{(2J+1)(2J-1)}} \quad (2)$$

for $P(\beta_{J, M}^{J-1, M})$ and $R(\beta_{J-1, M}^{J, M})$ branches of the rotational spectrum [23], as shown in Fig. 1. The electric dipole selection rules indicate that the rotational quantum number J changes by ± 1 for one-photon absorption, and $\Delta J = J'' - J = 0, 2$ and -2 correspond to Q , O , and S branches of the Raman spectrum, respectively.

A. STIRAP in a three-level system

The goal of STIRAP is to control the population transfer from the initial rovibrational state $|g\rangle = |\nu, J, M\rangle$ to the final

rovibrational state $|f\rangle = |\nu'', J'', M\rangle$ while keeping the population of the intermediate rovibrational state $|e\rangle = |\nu', J', M\rangle$ as small as possible. We summarize the standard three-level model of STIRAP [17]. The molecular wave function can be expanded as

$$|\Phi(t)\rangle = C_g(t)|g\rangle + C_e(t)|e\rangle + C_f(t)|f\rangle, \quad (3)$$

where, $C_g(t)$, $C_e(t)$, and $C_f(t)$ are the probability amplitudes of the three levels $|g\rangle$, $|e\rangle$, and $|f\rangle$, respectively. Using the time-dependent Schrödinger equation one can derive the coupled equation:

$$i\hbar \frac{\partial}{\partial t} \mathbf{C}(t) = \mathbf{H}(t) \mathbf{C}(t), \quad (4)$$

where $\mathbf{C}(t)$ is a three-component column matrix, with the elements $\{C_g(t), C_e(t), C_f(t)\}$. The Hamiltonian under rotation wave approximation (RWA) reads [25]

$$\mathbf{H}(t) = \hbar \begin{pmatrix} 0 & \frac{1}{2}\Omega_P(t) & 0 \\ \frac{1}{2}\Omega_P(t) & \Delta_P & \frac{1}{2}\Omega_S(t) \\ 0 & \frac{1}{2}\Omega_S(t) & \Delta_P - \Delta_S \end{pmatrix}. \quad (5)$$

Here Ω_P and Ω_S are the Rabi frequencies of the pump and Stokes pulses, respectively. $\hbar\Delta_P = E_e - E_g - \hbar\omega_P$ and $\hbar\Delta_S = E_e - E_f - \hbar\omega_S$ are the one-photon detunings of the pump and Stokes pulses from their respective transitions, respectively. An essential condition for STIRAP is the two-photon resonance, i.e., $\Delta_P = \Delta_S = \Delta$.

The theoretical treatment of STIRAP is greatly facilitated by introducing an adiabatic basis. It is straightforward to verify that the following linear combinations of the bare states $|g\rangle$, $|e\rangle$, and $|f\rangle$ are eigenstates of $\mathbf{H}(t)$:

$$|\Phi^+(t)\rangle = \sin \vartheta(t) \sin \varphi(t) |g\rangle + \cos \varphi(t) |e\rangle + \cos \vartheta(t) \sin \varphi(t) |f\rangle, \quad (6a)$$

$$|\Phi^0(t)\rangle = \cos \vartheta(t) |g\rangle - \sin \vartheta(t) |f\rangle, \quad (6b)$$

$$|\Phi^-(t)\rangle = \sin \vartheta(t) \cos \varphi(t) |g\rangle - \sin \varphi(t) |e\rangle + \cos \vartheta(t) \cos \varphi(t) |f\rangle, \quad (6c)$$

where the mixing angles $\vartheta(t)$ and $\varphi(t)$ are defined (modulo π) as $\vartheta(t) = \arctan[\Omega_P(t)/\Omega_S(t)]$ and $\varphi(t) = \frac{1}{2} \arctan[\sqrt{\Omega_P^2(t) + \Omega_S^2(t)}/\Delta]$. Instead of applying the pulses in the intuitive sequence, the Stokes pulse precedes the pump pulse. If the two pulses overlap sufficiently and are strong enough, $|\Phi^0(t)\rangle$ is an adiabatic dark state, and the population of the initial state $|g\rangle$ can be transferred completely to the target state $|f\rangle$. Thus, the time-dependent populations of $|g\rangle$ and $|f\rangle$ can be written as

$$P_g(t) = \cos^2 \vartheta(t), \quad P_f(t) = \sin^2 \vartheta(t). \quad (7)$$

B. STIRAP in molecular electronic states

In the present work, we describe STIRAP in molecular electronic states and do not invoke the RWA. Since the linearly polarized light is employed to excite the molecule, the quantum number M is conserved, i.e., $\Delta M=0$. The time-dependent wave function can be expressed as

$$\Phi_M(R, \theta, \phi, t) = e^{iM\phi} \Psi_M(R, \theta, t)/R, \quad (8)$$

where $\Psi_M(R, \theta, t)$ is calculated by

$$i\hbar \frac{\partial}{\partial t} \Psi_M(R, \theta, t) = \mathbf{H}(R, \theta, t) \Psi_M(R, \theta, t), \quad (9)$$

with

$$\Psi_M(R, \theta, t) = \begin{pmatrix} \psi_X(R, \theta, t) \\ \psi_A(R, \theta, t) \end{pmatrix}, \quad (10)$$

where $\psi_X(R, \theta, t)$ and $\psi_A(R, \theta, t)$ are the nuclear wave function in the electronic states X and A , respectively. The molecular Hamiltonian including the laser-molecule interaction is given by

$$\mathbf{H}(R, \theta, t) = (T_R + T_\theta) \mathbf{I} + \mathbf{W}(R, \theta, t), \quad (11)$$

where \mathbf{I} is a unit matrix, R is the internuclear separation, and θ is the angle between the molecular axis and the polarization direction of laser field, as shown in Fig. 1. The kinetic-energy terms are given by

$$T_R = -\frac{\hbar^2}{2m} \frac{\partial^2}{\partial R^2} \quad (12)$$

and

$$T_\theta = -\frac{\hbar^2}{2mR^2} \frac{1}{\sin \theta} \frac{\partial}{\partial \theta} \left(\sin \theta \frac{\partial}{\partial \theta} \right) + \frac{\hbar^2}{2mR^2} \frac{M^2}{\sin^2 \theta}, \quad (13)$$

where m represents the reduced mass of the molecule. If the laser pulse contains a resonant frequency of rovibrational transition, the first-order dipole interaction is dominant compared with the polarizability term [26], and therefore the laser-molecule interaction $\mathbf{W}(R, \theta, t)$ can be written as

$$\mathbf{W}(R, \theta, t) = \begin{pmatrix} V_X(R) & 0 \\ 0 & V_A(R) \end{pmatrix} - \epsilon(t) \cos \theta \times \begin{pmatrix} \mu_{XX}(R) & \mu_{XA}(R) \\ \mu_{XA}(R) & \mu_{AA}(R) \end{pmatrix}, \quad (14)$$

where $V_X(R)$ and $V_A(R)$ are the bare molecular potentials. $\mu_{ij}(R)$ ($i, j=X, A$) are the transition ($i \neq j$) and permanent ($i=j$) dipole moments at R .

Before propagating the time-dependent Schrödinger equation in Eq. (9), its initial form has to be defined. The initial wave packet is given by

$$\Psi_M(R, \theta, t=t_0) = \begin{pmatrix} \chi_{\nu J_0 M}(R) P_J^M(\cos \theta) \\ 0 \end{pmatrix}, \quad (15)$$

where $P_J^M(\cos \theta)$ is the associated Legendre polynomial and $\chi_{\nu J_0 M}(R)$ is J -dependent radial vibrational wave function. $P_J^M(\cos \theta)$ satisfy the following equation [27,28]:

$$\left[-\frac{1}{\sin \theta} \frac{\partial}{\partial \theta} \left(\sin \theta \frac{\partial}{\partial \theta} \right) + \frac{M^2}{\sin^2 \theta} - J(J+1) \right] P_J^M(\cos \theta) = 0. \quad (16)$$

Using Fourier grid Hamiltonian method [29], one can compute $\chi_{\nu J_0 M}(R)$ by solving numerically the radial Schrödinger equation,

$$\left[-\frac{\hbar^2}{2m} \frac{\partial^2}{\partial R^2} + V_X(R) + \frac{J(J+1)\hbar^2}{2mR^2} - \epsilon_{\nu J} \right] \chi_{\nu J_0 M}(R) = 0, \quad (17)$$

where $\epsilon_{\nu J}$ is the rovibrational energy of the ground electronic state X .

The time propagation is accomplished by using the split operator method [30,31]:

$$\begin{aligned} \Psi(R, \theta, t + \Delta t) &= U(\Delta t) \Psi(R, \theta, t) \\ &= e^{-(i/\hbar)\Delta t [T_R + T_\theta + \mathbf{W}(R, \theta, t)]} \Psi(R, \theta, t) \\ &\approx e^{-(i/2\hbar)\Delta t T_R} e^{-(i/2\hbar)\Delta t T_\theta} \\ &\quad \times e^{-(i/\hbar)\Delta t \mathbf{W}(R, \theta, t)} e^{-(i/2\hbar)\Delta t T_R} \\ &\quad \times e^{-(i/2\hbar)\Delta t T_\theta} \Psi(R, \theta, t). \end{aligned} \quad (18)$$

It is worth noting that the kinetic-energy operators, T_R and T_θ , are nonlocal in coordinate space. A basis-set expansion in the terms of the normalized associated Legendre polynomials are used to treat the angular part, and an evenly spaced grid is employed to calculate vibrational degree of freedom. Thus, in the calculation, T_R is transformed between momentum and coordinate spaces by using the fast Fourier transform method and T_θ is switched forward and backward between the polynomial representation and the coordinate space by utilizing discrete variable representation (DVR) technique [32]. The DVR is a unitary transformation of an finite basis representation (FBR) [33]. It is defined in terms of points η and weights ω_η of the N -point Gaussian quadrature associated with the orthogonal polynomial [34]:

$$T(\eta_i, J) = \sqrt{\omega_{\eta_i}} P_J^M(\cos \eta_i), \quad (19)$$

where η_i is a discrete angular basis. $W(R, \theta, t)$ acts on the wave function directly by multiplication in coordinate space.

The time-dependent population of the molecule in the electronic state $X(A)$ is computed by [35]

$$P_{X(A)} = \int d\theta \sin \theta \int dR |\psi_{X(A)}(R, \theta, t)|^2. \quad (20)$$

The time-dependent rovibrational population $P_{\nu_0 J_0 M}$ in the rovibrational eigenstate $\phi_{\nu_0 J_0 M} = \chi_{\nu_0 J_0}(R) P_{J_0}^M(\cos \theta)$ is calculated by [36]

$$P_{\nu_0 J_0 M}(t) = |\langle \phi_{\nu_0 J_0 M} | \Psi_M(R, \theta, t) \rangle|^2. \quad (21)$$

III. RESULTS AND DISCUSSION

In the calculation, we let R to vary in a range of 1.75–11.0 in atomic units with a 1024-point Fourier grid. The angular

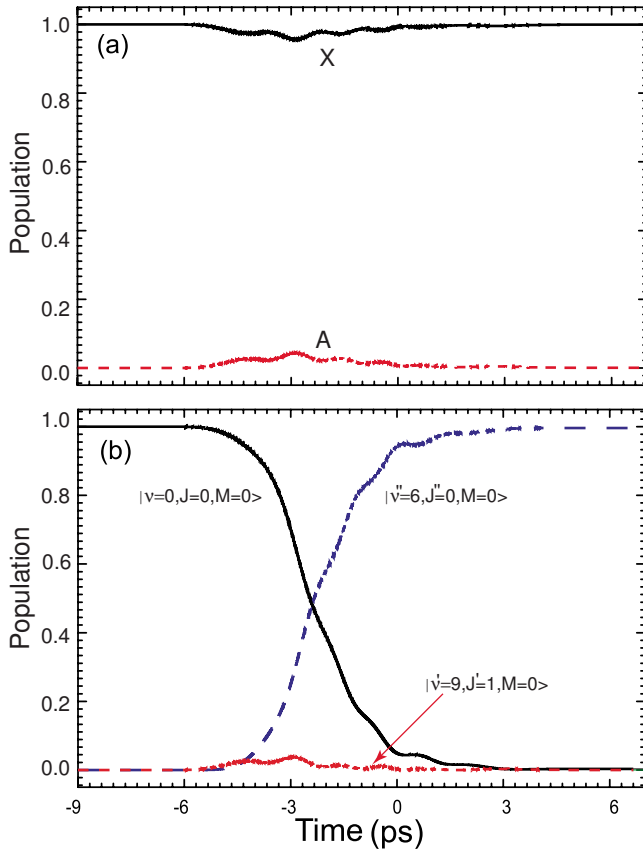


FIG. 2. (Color online) (a) The time-dependent population in the electronic states X and A. (b) The time-dependent rovibrational population in $|\nu=0, J=0, M=0\rangle$, $|\nu'=9, J'=1, M=0\rangle$, and $|\nu''=6, J''=0, M=0\rangle$. The laser parameters are chosen to be $I_p=3.1 \times 10^{10}$ W/cm², $I_S=2.32 \times 10^{10}$ W/cm², $\tau_p=\tau_S=5$ ps, $t_p=0$, $t_S=-2.5$ ps, $\hbar\omega_p=28\,954.37$ cm⁻¹, and $\hbar\omega_S=21\,482.29$ cm⁻¹.

grid points are 60 Gauss-Legendre quadrature points. The length of time step $\Delta t=0.05$ fs. The data of the two R -dependent potential-energy curves and the dipole moments are taken from Ref. [37]. A Gaussian pulse profile,

$$f_k(t) = e^{-4 \ln 2(t-t_k)^2/\tau_k^2}, \quad (22)$$

is employed throughout this work, where τ_k are full-widths at half-maximum (FWHMs) with $\tau_p=\tau_S=5.0$ ps. The pump pulse is centered at time $t_p=0$ ps, while the Stokes pulse with the center time $t_S=-2.5$ ps is applied before the pump pulse.

A. Rovibrational wave-packet manipulation via STIRAP using $|\nu=0, J=0, M=0\rangle$ as initial state

We consider a case in which the initial rovibrational state is $|g\rangle=|\nu=0, J=0, M=0\rangle$, the intermediate state $|e\rangle=|\nu'=9, J'=1, M=0\rangle$, and the target state $|f\rangle=|\nu''=6, J''=0, M=0\rangle$. The center frequency $\hbar\omega_p$ is 28 954.37 cm⁻¹ with the detuning $\hbar\Delta_p=-7$ cm⁻¹, and $\hbar\omega_S$ is 21 482.29 cm⁻¹ with the detuning $\hbar\Delta_S=-7$ cm⁻¹. The peak intensities of pump and Stokes pulses are 3.1×10^{10} W/cm² and 2.32×10^{10} W/cm², respectively. Figure 2 shows the time-

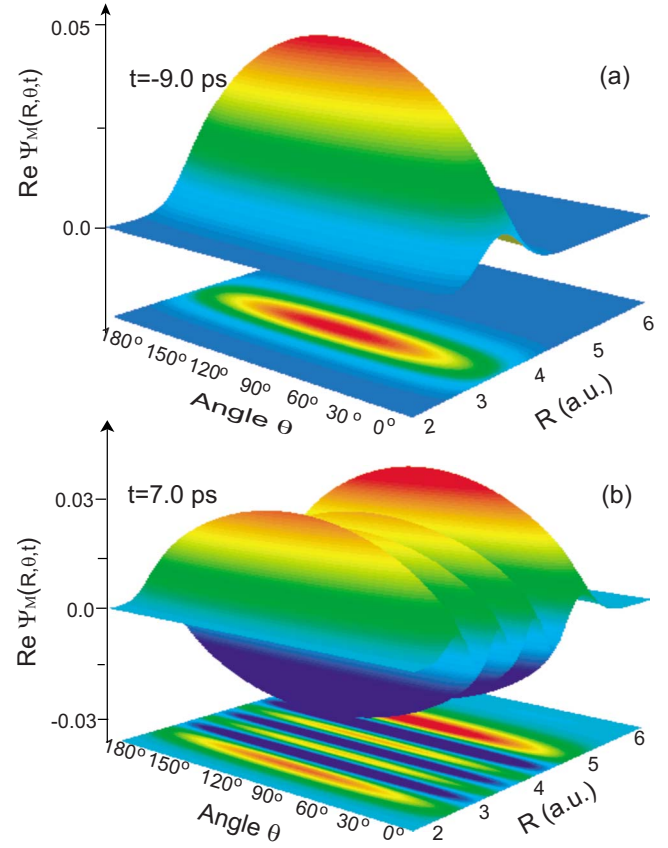


FIG. 3. (Color online) The real parts of the wave packet $\Psi_M(R, \theta, t)$ at (a) the initial time $t=-9.0$ ps and (b) the final time $t=7.0$ ps.

dependent populations in the electronic states X and A and the rovibrational states $|\nu=0, J=0, M=0\rangle$, $|\nu'=9, J'=1, M=0\rangle$, and $|\nu''=6, J''=0, M=0\rangle$. As can be seen in Fig. 2, the population almost completely stays in ground state X during the laser-molecule interaction, and the population on the excited state A is nearly the same as the rovibrational population on the state $|\nu'=9, J'=1, M=0\rangle$. This indicates that the population transfer process mainly takes place in the three rovibrational states $|g\rangle=|\nu=0, J=0, M=0\rangle$, $|e\rangle=|\nu'=9, J'=1, M=0\rangle$, and $|f\rangle=|\nu''=6, J''=0, M=0\rangle$ without involving other rovibrational states. A STIRAP relies on the existence of a dark state $|\Phi^0(t)\rangle$ in Eq. (6b). From Fig. 2(b), we can find that the time-dependent rovibrational population $P_{000}(t)$ on $|\nu=0, J=0, M=0\rangle$ decreases smoothly from 1 to 0, while $P_{600}(t)$ on $|\nu''=6, J''=0, M=0\rangle$ increases smoothly from 0 to 1. The population evolutions with time are well consistent with Eq. (7). Therefore, a STIRAP is successfully constructed in molecular electronic states.

Figure 3 displays the real parts of the wave packet $\Psi_M(R, \theta, t)$ at the initial time $t=-9.0$ ps and the final time $t=7.0$ ps. In Fig. 3(a), the initial wave packet is prepared on the rovibrational state $|\nu=0, J=0, M=0\rangle$. At the final time $t=7.0$ ps, the rovibrational wave packet in angular direction is very similar to the initial wave packet whose angular function is $P_0(\cos \theta)$, whereas in radial direction there are seven peaks which means $\nu''=6$. Therefore a rovibrational wave packet on the eigenstate $|\nu''=6, J''=0, M=0\rangle$ is obtained. As

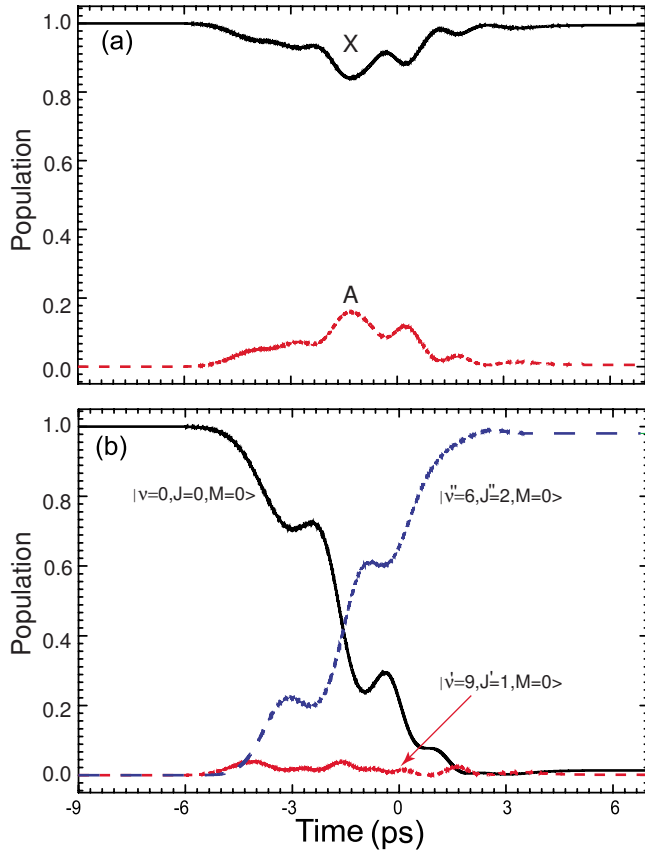


FIG. 4. (Color online) The time-dependent populations (a) in the electronic states X and A and (b) in the rovibrational states $|\nu=0, J=0, M=0\rangle$, $|\nu'=9, J'=1, M=0\rangle$, and $|\nu''=6, J''=2, M=0\rangle$. The peak intensities $I_p=3.1 \times 10^{10}$ W/cm² and $I_S=3.5 \times 10^{10}$ W/cm². The center frequencies $\hbar\omega_p=28\,947.37$ cm⁻¹ and $\hbar\omega_S=21\,438.29$ cm⁻¹.

can be seen in Fig. 3, the wave packet moves away from its initial region, and hence the molecular vibration and rotation should be taken into account.

In the above transition process, $\Delta J=J''-J=0$ corresponds to the Q branch of the Raman transition. We can also select the rovibrational state $|f\rangle=|\nu''=6, J''=2, M=0\rangle$ as the target state by the O branch of the Raman transition. Figure 4 shows the time-dependent populations in the electronic states X and A and the rovibrational states $|\nu=0, J=0, M=0\rangle$, $|\nu'=9, J'=1, M=0\rangle$, and $|\nu''=6, J''=2, M=0\rangle$. The center frequency $\hbar\omega_p$ is fixed at the transition frequency (28 947.37 cm⁻¹) of $|\nu'=9, J'=1, M=0\rangle \leftarrow |\nu=0, J=0, M=0\rangle$, and $\hbar\omega_S$ is equal to the transition frequency of $|\nu''=6, J''=2, M=0\rangle \leftarrow |\nu'=9, J'=1, M=0\rangle$. The peak intensities of pump and Stokes pulses are 3.1×10^{10} and 3.5×10^{10} W/cm², respectively. From Fig. 4(b), we find that the population can be transferred completely from $|\nu=0, J=0, M=0\rangle$ to $|\nu''=6, J''=2, M=0\rangle$. Figure 5 shows the real part of $\Psi_M(R, \theta, t)$ at $t=7.0$ ps, and the Legendre function $P_2(\cos \theta)$. The distribution of rovibrational wave packet in angle direction is very similar to the curve of $P_2(\cos \theta)$. In radial direction there are seven peaks. Therefore, the population of the initial state is transferred to the rovibrational state $|\nu''=6, J''=2, M=0\rangle$.

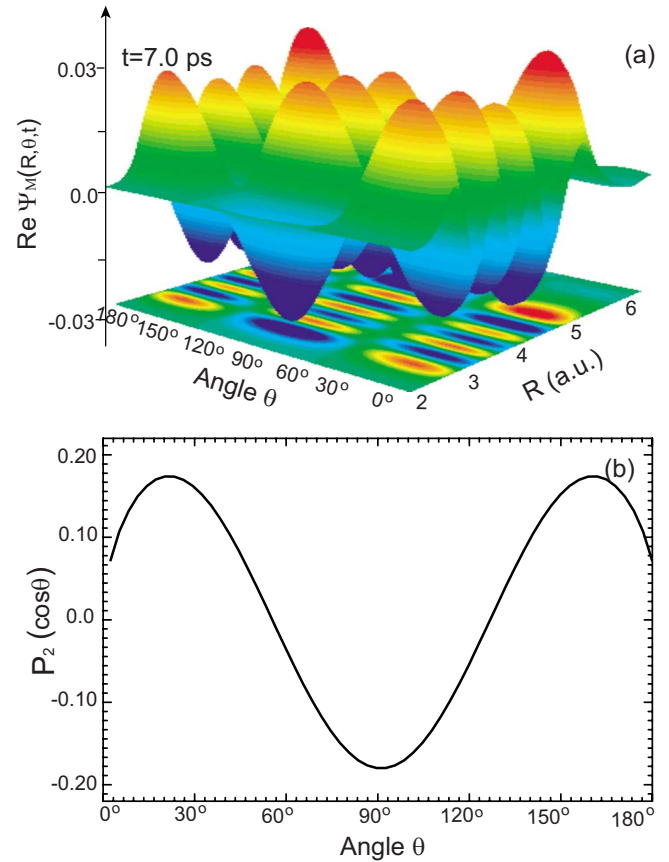


FIG. 5. (Color online) (a) The real part of the wave packet $\Psi_M(R, \theta, t)$ at the final time $t=7.0$ ps and (b) the Legendre function $P_2(\cos \theta)$.

Besides the above three rovibrational states, a small amount population can be transferred to other rovibrational states. From Fig. 4, we can see that the population P_A on the excited state A is evidently larger than rovibrational population P_{910} on $|\nu'=9, J'=1, M=0\rangle$. This indicates that the other rovibrational states take part in the excitation process, and the nonadiabatic coupling happens. There are two possibilities to increase the population of the excited state A. First, the population may be transferred from the final state $|\nu''=6, J''=2, M=0\rangle$ to the excited state A by the pump and Stokes pulses. Second, the two-photon or multiphoton transition path between the X and A states can be opened because of the mixed parity in at least one of the two levels for a polar molecule [38,39]. As can be seen in Fig. 4(a), the population on the excited state A reaches its peak value at $t=-1.35$ ps. To explore the population transfer mechanism in Fig. 4, we depict the real part of wave packet $\psi_A(R, \theta, t)$ at $t=-1.35$ ps and the Legendre function $P_3(\cos \theta)$ in Fig. 6. The distribution of the rovibrational wave packet in angle direction is in conformity with the curve of $P_3(\cos \theta)$, and there are ten clear peaks in radial direction. Thus, we can infer that the rovibrational state $|\nu'=9, J'=3, M=0\rangle$ is coupled by Stokes pulse, corresponding to the $\Delta J=J'-J''=1$ transition.

In order to explore the detail of the effect of the others states on the population dynamics, we present the time-dependent population distributions on the excited state A and

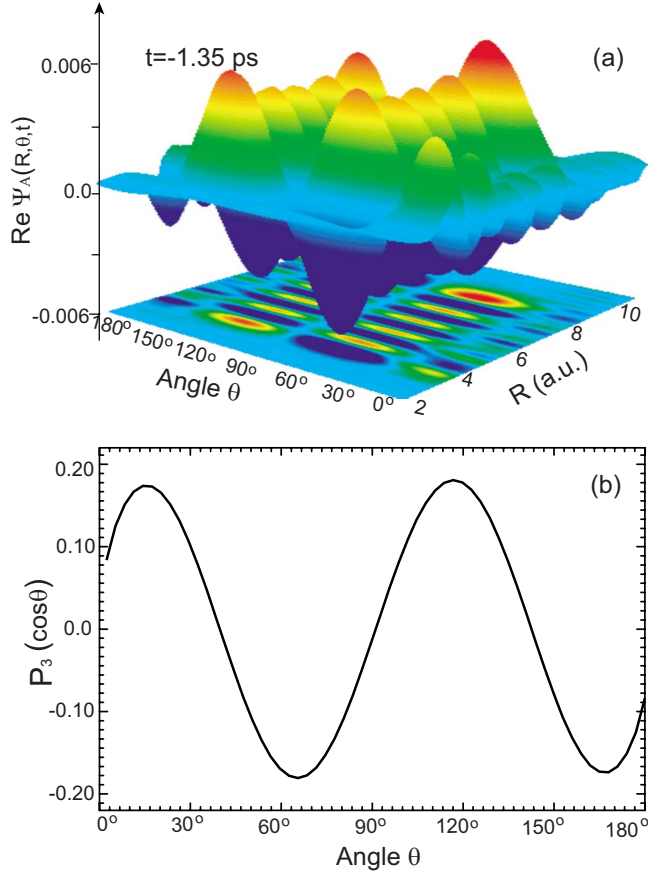


FIG. 6. (Color online) (a) The real part of the wave packet $\psi_A(R, \theta, t)$ at $t = -1.35$ ps and (b) the Legendre polynomial $P_3(\cos \theta)$.

the related rovibrational states in Fig. 7. The sum of the populations on $|\nu' = 9, J' = 1, M = 0\rangle$ and $|\nu' = 9, J' = 3, M = 0\rangle$ is nearly equal to the total population on the excited state A. Therefore, the first population transfer path induced by the Stokes pulse is dominant, and the second population transfer path is eliminated. However, if the intensities of laser pulses become intense, and the multiphoton resonant condition is satisfied, the second population transfer path will become

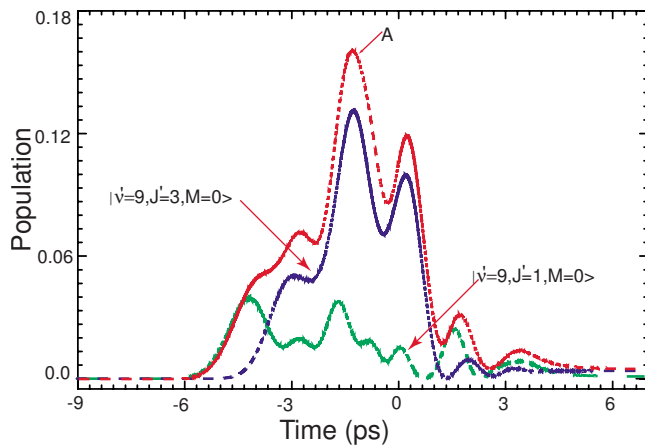


FIG. 7. (Color online) The time-dependent populations on the excited state A and the related rovibrational states.

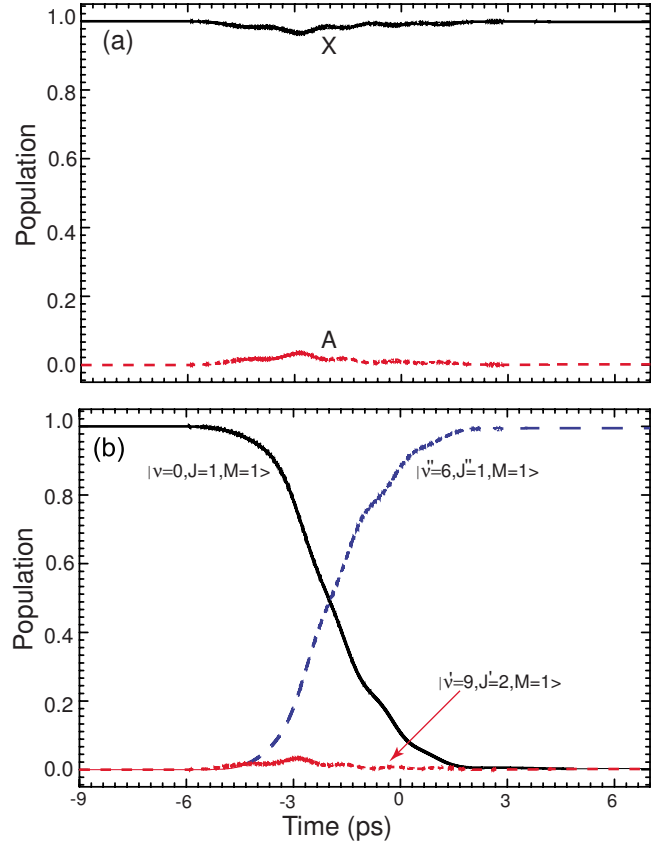


FIG. 8. (Color online) (a) The time-dependent populations in the electronic states X and A and (b) the time-dependent rovibrational populations in $|\nu = 0, J = 1, M = 1\rangle$, $|\nu' = 9, J' = 2, M = 1\rangle$, and $|\nu'' = 6, J'' = 1, M = 1\rangle$. The center frequency $\hbar\omega_p$ is $28\,951.61\text{ cm}^{-1}$ with the detuning $\hbar\Delta_p = 8\text{ cm}^{-1}$, and $\hbar\omega_s$ is $21\,482.07\text{ cm}^{-1}$ with the detuning $\hbar\Delta_s = -8\text{ cm}^{-1}$. The peak intensities of pump and Stokes pulses are 3.5×10^{10} and $3.9 \times 10^{10}\text{ W/cm}^2$, respectively.

important for the increase in the excited-state population [38,39].

B. Rovibrational wave-packet manipulation via STIRAP using $|\nu = 0, J = 1, M = 1\rangle$ as initial state

We have performed the calculations using the ground rovibrational state as initial state, where the quantum number $M = 0$. We now present the calculated result using $|\nu = 0, J = 1, M = 1\rangle$ as initial state. According to the selection rules $\Delta J = \pm 1$ and $\Delta M = 0$, the intermediate state $|e\rangle$ should be $|\nu' = 9, J' = 2, M = 1\rangle$ and the target state $|f\rangle$ may be $|\nu'' = 6, J'' = 1, M = 1\rangle$ or $|\nu'' = 6, J'' = 3, M = 1\rangle$. Figure 8 shows the time-dependent population distribution when $|\nu'' = 6, J'' = 1, M = 1\rangle$ is taken as the target state. The center frequency $\hbar\omega_p$ is $28\,951.61\text{ cm}^{-1}$ with detuning $\hbar\Delta_p = -8\text{ cm}^{-1}$, and $\hbar\omega_s$ is $21\,482.07\text{ cm}^{-1}$ with detuning $\hbar\Delta_s = -8\text{ cm}^{-1}$. The peak intensities of pump and Stokes pulses are 3.5×10^{10} and $3.9 \times 10^{10}\text{ W/cm}^2$, respectively. From Fig. 8(b), we can see that the rovibrational population is nearly 100% transferred from the initial state $|\nu = 0, J = 1, M = 1\rangle$ to the final state $|\nu'' = 6, J'' = 1, M = 1\rangle$, and the intermediate state $|\nu' = 9, J' = 2, M = 1\rangle$ is almost unpopulated. As can be seen in Fig. 8, the

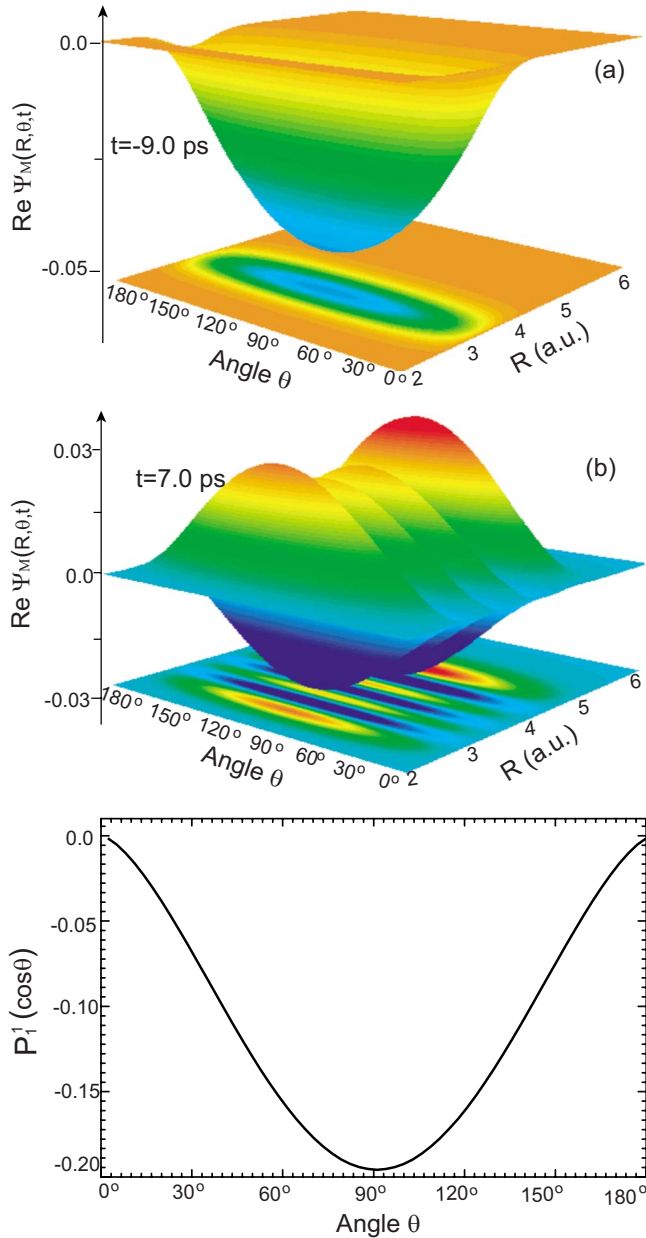


FIG. 9. (Color online) (a) The real part of the wave packet $\Psi_M(R, \theta, t)$ at $t = -9.0$ ps, (b) the real part of the wave packet $\Psi_M(R, \theta, t)$ at $t = 7.0$ ps, and (c) the associated Legendre polynomial $P_1^1(\cos \theta)$.

population on the rovibrational state $|\nu' = 9, J' = 2, M = 1\rangle$ is very close to the population on the excited state A. This means that the effect of the other states on the STIRAP process is very small. The population is adiabatically transferred from the initial rovibrational state $|\nu = 0, J = 1, M = 1\rangle$ to a superposition of the states $|\nu = 0, J = 1, M = 1\rangle$ and $|\nu' = 9, J' = 2, M = 1\rangle$ during the laser-molecule interaction and finally to the target state $|\nu'' = 6, J'' = 1, M = 1\rangle$. Figure 9 shows the real parts of the wave packet $\Psi_M(R, \theta, t)$ at $t = -9.0$ and 7.0 ps and the function $P_1^1(\cos \theta)$. We can see that the wave packet moves perfectly from the initial state $|\nu = 0, J = 1, M = 1\rangle$ to the target state $|\nu'' = 6, J'' = 1, M = 1\rangle$ after the interaction is over.

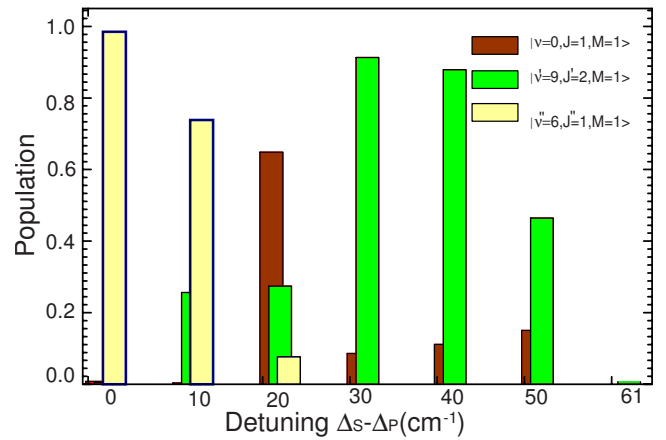


FIG. 10. (Color online) The final rovibrational populations in the rovibrational states $|\nu = 0, J = 1, M = 1\rangle$, $|\nu' = 9, J' = 2, M = 1\rangle$, and $|\nu'' = 6, J'' = 1, M = 1\rangle$ for different two-photon detunings $\Delta_S - \Delta_P$ with fixed one-photon detuning $\Delta_P = 0$.

The STIRAP is very sensitive to the two-photon detuning. In Figs. 2 and 8, we have depicted the population transfer processes in the case of one-photon detuning and two-photon resonance. In the following, we discuss the influence of two-photon detuning on the STIRAP in molecular electronic states. Figure 10 shows the final rovibrational populations in the rovibrational states $|\nu = 0, J = 1, M = 1\rangle$, $|\nu' = 9, J' = 2, M = 1\rangle$, and $|\nu'' = 6, J'' = 1, M = 1\rangle$ for different two-photon detunings $\Delta_S - \Delta_P$, where the one-photon detuning $\Delta_P = 0$, and the other laser-pulse parameters are the same as those in Fig. 9. We can see that the final population is very sensitive to the two-photon detuning. Especially at two-photon detuning $\hbar\Delta_S - \hbar\Delta_P = 61$ cm $^{-1}$, the three rovibrational states are almost unpopulated. The population is completely transferred to the other rovibrational states. To search the “lost” population, in Fig. 11, we present the real part of $\Psi_M(R, \theta, t)$ at $t = 7.0$ ps and the function $P_3^1(\cos \theta)$. We can see that the wave packet is almost located in an eigenstate. The real part of $\Psi_M(R, \theta, t)$ in angular direction is very similar to the function $P_3^1(\cos \theta)$, and there are seven peaks in radial direction. Therefore, the lost population is searched on the rovibrational state $|\nu'' = 6, J'' = 3, M = 1\rangle$ which corresponds to the *O* branch of Raman transition. In the typical multilevel STIRAP model, however, one must take enough levels into account to solve this problem. Thus, our treatment possesses an evident advantage for the complicated situation where other rovibrational states participate in the population transfer process.

From the above discussions, we can conclude that the desired target state can be selected by adjusting laser-pulse parameters, but the two-photon resonance must be maintained. Goto and Ichimura [15] demonstrated that if the variation in the Rabi frequency is sufficiently slow, and two-photon detunings are small compared with the Rabi frequencies, the adiabatic approximation with two dark states is valid, and consequently the population transfer process can be regarded as tripod STIRAP via the two dark states even in the presence of small two-photon detunings. Based on this approach, we can extend our method to investigate the tripod STIRAP in molecular electronic states with small two-photon detunings by adding a laser pulse.

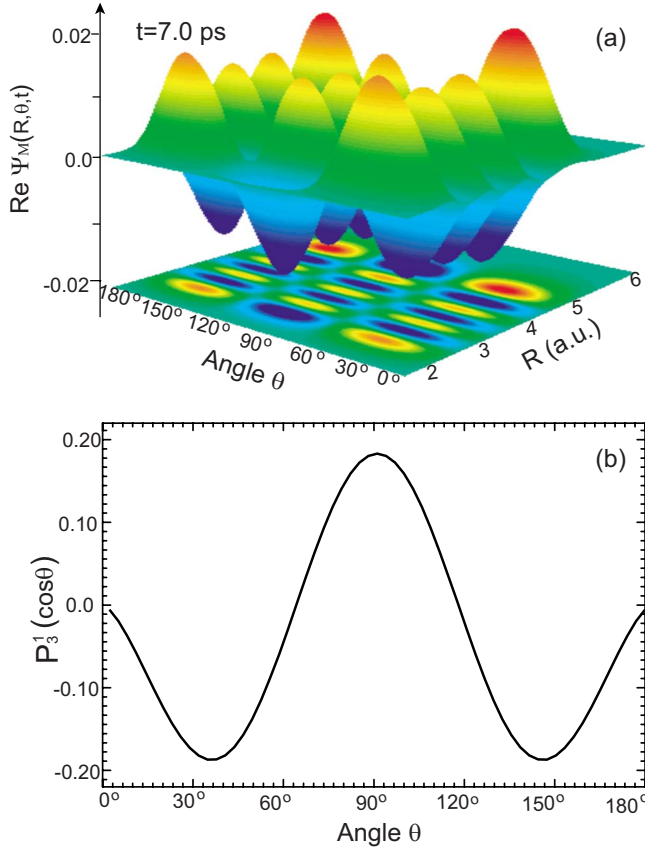


FIG. 11. (Color online) (a) The real part of the wave packet $\Psi_M(R, \theta, t)$ at the final time $t=7.0$ ps and (b) the associated Legendre polynomial $P_3^1(\cos \theta)$.

C. Rovibrational wave-packet manipulation via STIRAP using thermal mixed state as initial state

We now present the calculated results using thermal mixed state as initial state. Considering the effect of the temperature is equivalent to statistically averaging over the solutions of the Schrödinger equation for all possible initially rovibrational states weighed by a Boltzmann factor $\sqrt{P(\nu, J)}$ [28,40]. Since we consider only the case of low temperature, the statistically averaging over vibrational quantum numbers ν is omitted. The Boltzmann distribution $P(\nu, J)$ associated with the rotational states is given by

$$P(\nu, J) = \frac{1}{Q} \exp\left[\frac{-BJ(J+1)}{\kappa_B T}\right], \quad (23)$$

where

$$Q = \sum_{J=0}^{\infty} (2J+1) \exp\left[\frac{-BJ(J+1)}{\kappa_B T}\right] \quad (24)$$

is the partition function. B , κ_B , and T are the molecular rotation constant, the Boltzmann constant, and the rotational temperature, respectively.

For simplicity but without loss of generality, we consider a case at rotational temperature $T=20$ K, where only initial rotational states of $J=0$ and 1 make a significant contribution. The initial state of $J=1$ contains the rovibrational states

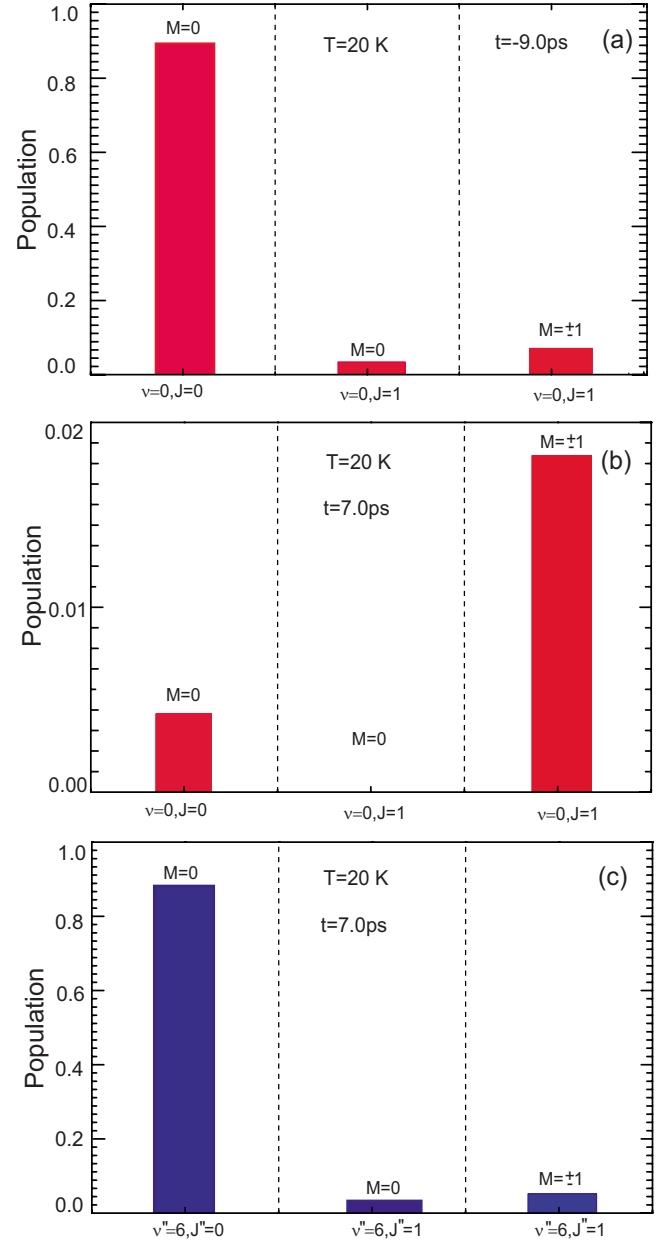


FIG. 12. (Color online) The thermally rovibrational populations (a) at $t=-9.0$ ps, [(b) and (c)] at $t=7.0$ ps. The pulse parameters are the same as those in Fig. 2.

$|\nu=0, J=1, M=0\rangle$ (statistical weight of 1/3) and $|\nu=0, J=1, M=\pm 1\rangle$ (statistical weight of 2/3). Each of them has to be propagated separately and then combined by using the respective weights. Figure 12 shows the thermally rovibrational populations at $t=-9.0$ and 7.0 ps with the same pulse parameters as those in Fig. 2. When the molecule is initially in a thermal mixed state, the population of the initial state can be transferred to the target state through the different branches of Raman transition. However, it is difficult to transfer full population from the thermally mixed state to the target state via a STIRAP because different rovibrational levels of the thermally initial state correspond to different two-photon resonant conditions. As can be seen in Fig. 12, the efficiency of population transfer is lower than that using a

pure adiabatic states as initial state. According to Eqs. (2) and (16), for a given J , all rotational states $|J, M\rangle$ are degenerate in energy, but the M quantum number influences the strength of coupling. From Fig. 12, we can find that the efficiency of population transfer from $|\nu=0, J=1, M=0\rangle$ to the target state is evidently higher than that from $|\nu=0, J=1, M=\pm 1\rangle$ because the Rabi frequency for $M=0$ is larger than that for $M=\pm 1$.

IV. CONCLUSION

We have investigated the rovibrational dynamics of STIRAP in the molecular electronic states including both the rotational and the vibrational degrees of freedom, with the LiH molecule as the example. Using a pure rovibrational state as the initial state, we have found that, under the condition of the two-photon resonance, the population can be transferred to the selective rovibrational state, and the target state can be controlled by adjusting laser-pulse parameters. Besides the interested rovibrational states, we have noticed that some unwanted rovibrational states affect the dynamics of STIRAP, especially while the condition of the two-photon resonance was broken. Our calculations show that the rota-

tional and the vibrational degrees of freedom should not be ignored when we construct a STIRAP in molecular electronic states. By inspecting the evolution process of wave packet, we can easily visualize the nuclear motion and the underlying physics and explore the effect of the unwanted rovibrational states on the population transfer. When the initial state of the LiH molecule is a thermal mixed rovibrational state, it is difficult to transfer full population from the thermally mixed state to the target state via a STIRAP and the efficiency of population transfer was lowered in a certain degree because different rovibrational levels of the thermally initial state correspond to different two-photon resonant conditions. In the present work, we only consider the one-photon coupling between the two electronic states. The theoretical treatment can be easily extended to the case of multiphoton coupling and can also be applied to other diatomic molecules. Naturally, a comparison of the theoretical results with experimental data is very desirable.

ACKNOWLEDGMENT

This work was supported by the National Science Foundation of China under Grants No. 10674022 and No. 20633070.

-
- [1] H. G. Rubahn and K. Bergmann, *Annu. Rev. Phys. Chem.* **41**, 735 (1990).
- [2] A. Ekert and R. Jozsa, *Rev. Mod. Phys.* **68**, 733 (1996).
- [3] M. Weitz, B. C. Young, and S. Chu, *Phys. Rev. Lett.* **73**, 2563 (1994).
- [4] V. S. Malinovsky and I. R. Solá, *Phys. Rev. Lett.* **93**, 190502 (2004).
- [5] T. Cubel, B. K. Teo, V. S. Malinovsky, J. R. Guest, A. Reinhard, B. Knuffman, P. R. Berman, and G. Raithel, *Phys. Rev. A* **72**, 023405 (2005).
- [6] S. D. Clow, C. Trallero-Herrero, T. Bergeman, and T. Weinacht, *Phys. Rev. Lett.* **100**, 233603 (2008).
- [7] E. A. Shapiro, A. Péer, J. Ye, and M. Shapiro, *Phys. Rev. Lett.* **101**, 023601 (2008).
- [8] M. Shapiro and P. Brumer, *Rep. Prog. Phys.* **66**, 859 (2003).
- [9] D. J. Tannor, R. Kosloff, and S. A. Rice, *J. Chem. Phys.* **85**, 5805 (1986).
- [10] K. Bergmann, H. Theuer, and B. W. Shore, *Rev. Mod. Phys.* **70**, 1003 (1998).
- [11] L. P. Yatsenko, B. W. Shore, T. Halfmann, K. Bergmann, and A. Vardi, *Phys. Rev. A* **60**, R4237 (1999).
- [12] B. M. Garraway and K. A. Suominen, *Phys. Rev. Lett.* **80**, 932 (1998).
- [13] U. Gaubatz, P. Rudecki, M. Becker, S. Schiemann, M. Külz, and K. Bergmann, *Chem. Phys. Lett.* **149**, 463 (1988).
- [14] U. Gaubatz, P. Rudecki, S. Schiemann, and K. Bergmann, *J. Chem. Phys.* **92**, 5363 (1990).
- [15] H. Goto and K. Ichimura, *Phys. Lett. A* **372**, 1535 (2008).
- [16] A. Brown, *Chem. Phys.* **342**, 16 (2007).
- [17] N. V. Vitanov and B. W. Shore, *Phys. Rev. A* **73**, 053402 (2006).
- [18] P. D. Drummond, K. V. Kheruntsyan, D. J. Heinzen, and R. H. Wynar, *Phys. Rev. A* **65**, 063619 (2002).
- [19] M. Tsubouchi, A. Khramov, and T. Momose, *Phys. Rev. A* **77**, 023405 (2008).
- [20] M. Tsubouchi and T. Momose, *Phys. Rev. A* **77**, 052326 (2008).
- [21] E. W. Lerch, X.-C. Dai, E. A. Torres, J. B. Ballard, H. U. Stauffer, and S. R. Leone, *J. Phys. B* **41**, 074015 (2008).
- [22] C.-C. Shu, K.-J. Yuan, W.-H. Hu, J. Yang, and S.-L. Cong, *Phys. Rev. A* **78**, 055401 (2008).
- [23] B. Y. Chang and I. R. Solá, *Chem. Phys.* **338**, 228 (2007).
- [24] S. Gräfe, W. Kiefer, and V. Engel, *J. Chem. Phys.* **127**, 134306 (2007).
- [25] N. V. Vitanov, T. Halfmann, B. W. Shore, and K. Bergmann, *Annu. Rev. Phys. Chem.* **52**, 763 (2001).
- [26] E. Gershnabel, I. Sh. Averbukh, and R. J. Gordon, *Phys. Rev. A* **74**, 053414 (2006).
- [27] M. Machholm and N. E. Henriksen, *J. Chem. Phys.* **111**, 3051 (1999).
- [28] M. Machholm and N. E. Henriksen, *Phys. Rev. Lett.* **87**, 193001 (2001).
- [29] C. C. Marston and G. G. Balint-Kurti, *J. Chem. Phys.* **91**, 3571 (1989).
- [30] M. D. Feit, *J. Chem. Phys.* **78**, 301 (1983).
- [31] Y.-C. Han, K.-J. Yuan, W.-H. Hu, T.-M. Yan, and S.-L. Cong, *J. Chem. Phys.* **128**, 134303 (2008).
- [32] D. Kosloff and R. Kosloff, *J. Comput. Phys.* **52**, 35 (1983).
- [33] J. C. Light and I. P. Hamilton, *J. Chem. Phys.* **82**, 1400 (1985).
- [34] Z. Bačić and J. C. Light, *Annu. Rev. Phys. Chem.* **40**, 469 (1989).

- [35] K.-J. Yuan, Z. Sun, S.-L. Cong, and N. Lou, *Phys. Rev. A* **74**, 043421 (2006).
- [36] P. Marquetand and V. Engel, *J. Chem. Phys.* **127**, 084115 (2007).
- [37] H. Partridge and S. R. Langhoff, *J. Chem. Phys.* **74**, 2361 (1981).
- [38] C.-C. Shu, K.-J. Yuan, W.-H. Hu, and S.-L. Cong, *J. Phys. B* **41**, 065602 (2008).
- [39] W.-F. Yang, S.-Q. Gong, R.-X. Li, and Z.-Z. Xu, *Phys. Rev. A* **74**, 013407 (2006).
- [40] J. Salomon, C. M. Dion, and G. Turinici, *J. Chem. Phys.* **123**, 144310 (2005).